Fully Integrated Solution for LWD Resistivity Image Application a case study from Beibu Gulf, China

Lei Xiao, Cai Jun, CNOOC; Yang Shi Duo, Shim Yen Han, Wu Hong Xia and Wang Yu Xi Schlumberger

This paper was prepared for presentation at the 1st SPWLA India Regional Conference, Formation Evaluation in Horizontal Wells, Mumbai, March 19 - 20, 2007.

ABSTRACT

This carbonate field was discovered in 1987 by China National Offshore Oil Corporation, CNOOC. It is located in the BeiBu Gulf of the South China Sea. The depositional environment is an open platform bounded by high-water-flow.

Recently, two horizontal development wells were drilled in this oilfield to enhance the oil production. They were logged with adnVISION* (ADN) and geoVISION* (GVR) logging while drilling (LWD) tools. To fully understand the structure and fracture system of the area, an integrated solution using GVR resistivity images was initiated. This study includes structural, stratigraphic and stress analysis, and quantitative fracture and secondary porosity computation.

Based on the structural analysis, the NE-SW near-borehole structure could be confirmed. Combining the fracture strike statistics and local structure, the fracture development principle was analyzed. In addition, the fracture porosity was calculated using the dual laterolog resistivity algorithm (Pezard & Anderson, 1990).

Secondary porosity was computed from the GVR images by adapting a method originally developed for use with wireline images. A Vug Multiple Effect Factor (V_m) was introduced to generate a porosity map around the borehole using the azimuthal resistivity data obtained from GVR. Using this porosity map, windowed over short intervals, Porosity Spectrum Analysis (PoroSpect)* was used to provide a continuous output of the primary and secondary porosity components for the whole logging interval.

With the combination of GVR resistivity images and density neutron data, a fully integrated solution was performed to better define the lithology, geological structure, petrophysical properties and geomechanic analysis.

INTRODUCTION

This marginal field is located in the Beibu Gulf with water depth from 30 to 150 meters. The current field production is between 2,000 to 3,000 barrels of oil per day with expected 3,700 barrels of oil per day at its peak from one unmanned wellhead platform. Since 1987, five wells have been drilled. Of these five, three were exploration and two were horizontal development wells. Of the three exploration wells, two were good prospects and are both currently on production (Figure 1).

The depositional environment of carbonate is an open platform. The main reservoir zone is located in the lower Tertiary Liushagang Formation Third Unit, Carboniferous carbonate. The lithology of this formation consists of fine-middle sandstone and grey carbonate conglomerate; the major composition of the conglomerate is limestone or dolomite. The Carboniferous pay zone includes limestone, skeletal grain and secondary dolomite (Figure 2). The fractures are very developed in the carbonate, and most of the fractures are filled by calcite.

The weathered zone has high uncertainty, which was only identified in one of the exploration wells. The porosity of the weathered zone is 16% and of the carbonate it is 5.8%. The reservoir has a unified pressure system.

The most recent two horizontal development wells, A1H and A2H, were drilled in 2006. The objective of the wells was to drill through the weathered zone of carbonate conglomerate and into the carbonate formation. Because of high borehole stability risk in the weathered zone, special considerations were taken to select a suitable logging program.

LOGGING TOOL SELECTION

There were two main requirements identified to successfully log these wells: Firstly, to obtain geological and petrophysical data prior to the deterioration of the borehole in the weathered zone; and secondly, to secure good quality log data before any alteration occurred around the borehole in the reservoir

* Mark of Schlumberger

section. Based on these reasons, measurement while drilling (MWD) and LWD tools were selected as the primary logging instruments to acquire all necessary data in real-time while drilling. In addition, this technology provides the capability for proactive geosteering to place the well in the targeted reservoir with limited offset well information.

The final LWD tools chosen were the GVR, MWD and ADN. A short description of each tool together with the measurements they provide is given below:

The **GVR** provides azimuthal formation gamma ray and five laterolog resistivity measurements. Resistivity-at-bit provides the first indication of a lithology change, Ring resistivity provides a deep focused resistivity measurement, and three azimuthal button resistivities measure 56 resistivity values per rotation for each button at three different depth of investigation. These three buttons also provide three distinct resistivity images around the borehole while the tool is in rotation.

The **MWD** tool provides inclination and azimuthal measurements for directional survey computation and also collects downhole drilling and formation evaluation information, including images, from all the tools in the bottom hole assembly (BHA). This data is then transmitted to the surface using mud pulse telemetry. At the same time, the tool generates power from the mud passing through it to power the tools in the BHA.

The **ADN** provides bulk density, thermal neutron porosity and ultrasonic caliper measurements. Like the GVR, the ADN also provides azimuthal measurements. The density, Pef and ultrasonic caliper data can be provided azimuthally in both memory and real-time mode. However, due to the high borehole stability risk in the weathered zone, this tool was not picked up until after the well was drilled to TD, and the data was reacquired in a reaming mode.

FULLY INTEGRATED SOLUTION

Borehole images have become the major source of geological information from logging data since 1986. Currently there are relatively few ways of acquiring borehole images; most commonly used are the resistivity images acquired with either wireline tools such as the Formation MicroImager (FMI)* or LWD tools such as the GVR.

The resolution difference between these two types of images determines the extent of geological interpretation that can be offered. The high-resolution image provided by the wireline electrical image can describe rock texture, rock composition, and sedimentary features. The GVR images have a lower resolution and their use is normally limited to formation dip estimation and structural analysis, and fracture identification.

With the latest enhanced image resolution, GVR resistivity images used in combination with ADN measurements can provide an integrated solution to better define the geological structural environment and improve the petrophysical evaluation beyond what is currently available in the market.

GEOLOGICAL APPLICATION

Lithology classification. In general, lithology identification in horizontal wells is relatively straightforward with a simple well design type that targets a single lithology. However, in complex structures or thin-bedded stratigraphic areas, the lithology classification can become very challenging. In this situation, lithology classification can very often not be completed by the use of images alone. Additional core data and/or cuttings information and other petrophysical data need to be evaluated for proper classification.

The Neural Network (NN) classification can be considered as a software implementation of the methodology that was originally performed by comprehensive manual methods. The first step is establishing a GVR image pattern by comparing each feature with existing core or cuttings information. Then, according to petrophysical parameters, decide on the appropriate properties that characterize the core or cuttings. These properties depend on the logging tool used: GVR - resistivity and GR measurements; ADN - density, neutron porosity, PEF, and caliper measurements. Finally, through on iterative process of comparing computed lithology with core or cutting, the optimum scheme for evaluating lithology from log data is obtained. This process is illustrated in the flowchart shown in Figure 4.

Based on the special characteristics of each formation type, there were four different lithologies identified in this well; shale, chalk shale, sand, and carbonate. The final classification result for well A2H is shown in Figure 5.

Shale has high GR, high density and neutron porosity, low resistivity, and appears as a darker brown color in the static resistivity images. From the images, the bed boundaries are very clear and in some sections formation deformation is also visible.

Chalk shale has a relatively high GR, medium resistivity, and appears as a brown color in the static resistivity image. A few of these bed boundaries can be identified from the GVR images.

Sand has a similar log response to the chalk shale. However, it has a low GR and high resistivity response that appears as a yellow color in the static images.

Carbonate has a different signature compared to those above; it has lower GR, higher density, lower neutron porosity, relatively higher resistivity and appears as a bright color in the static images with fracture features visible in the images.

Structural Analysis. From the close-up GVR image, formation bed boundaries can be distinguished in the shale and chalk shale formations. Dip picking was made following these sinusoidal features (Figure 7). In some cases, deformation of the structure was also identified through images as shown in Figure 9. These features provide additional information for formation structure and facies analysis. The darker color of the image represents low resistivity measurements while the lighter color represents high resistivity measurements.

Based on the dips picked on the images from shale formations, the cross-well structure could be interpreted as shown in Figure 6. Based on this study, the azimuth of the structure was presented as SE, with 10° to 20° dip, confirming the initial structure from the map (Figure 1).

PETROPHYSICAL ANALYSIS

Fracture Analysis. From the LWD resistivity image, there are three fracture zones identified: A breccia zone (Figure 8), a fractured carbonate zone with interbedded tight features (Figure 10), and a fractured carbonate zone (Figure 11). The breccia zone is located at the top of the carbonate; picking fractures in this zone is very difficult because of the shape of irregular rock fragments. However, the features of fractured carbonate zones can be easily identified and picked, especially zones with interbedded tight features.

The dual laterolog response in fractured rocks was first introduced by Sibbit and Faivre (1985). There are two major simplifying assumptions used for fracture analysis; high formation contrast compared to mud resistivity ($R_t >> R_m$), and the separation between deep laterolog resistivity (LLD) and shallow laterolog resistivity (LLS) is due to invasion. Pezard and Anderson (1990) extend their work to include the influence of the fracture angle. They proposed the fracture porosity algorithms:

$$
\begin{aligned}
&\textit{if } (LLD > LLS) \\
&\quad \Phi_f = (1/LLS^{\wedge 2} - 1/LLD^{\wedge 2}) \times R_{mf} \times LLD \times 200 \\
&\textit{if } (LLS > LLD) \\
&\quad \Phi_f = (1/LLD^{\wedge 2} - 1/LLS^{\wedge 2}) \times R_{mf} \times LLD \times 100
\end{aligned}
\qquad (1)
$$

Where

Φ_f is the fracture porosity, %
R_{mf} is the mud filter resistivity, ohm.m.

The GVR provides multi-depth focused laterolog resistivity measurements. In the LWD logging environment, with little or slight invasion in permeable zones, the deep button resistivity and ring resistivity are almost the same; the shallow button might be affected by invasion or influenced by irregular borehole geometry. Thus, for this study, the deep and medium button resistivity measurements have been selected with the assumption that fractures are the major cause of separation between middle button and deep button resistivities. Based on this assumption, quantitative computation of fractures is carried out. Combining fracture density, length and porosity, the zone with developed fractures can be quickly identified. For example, in A1H well, the fractured carbonate is very developed in all intervals with a fracture density around 0.6#/m, length 1.578m/m^2 and porosity 0.03%. These results are shown in Figure 12 and Figure 16.

Secondary porosity analysis. It is well known that correlations between hydrocarbon production and neutron-density logs can be inconsistent for some reservoirs. In carbonate formations with inherent azimuthal anisotropy and lateral heterogeneity, it is often found that good production can be obtained from intervals showing low log porosity readings whereas zones with higher log porosity may not produce as expected.

To get a better understanding of the structure and a better estimate of carbonate reservoir production, the high resolution wireline electrical image was used to compute the secondary porosity (Newberry, 1996), while the Combinable Magnetic Resonance tool (CMR)* provided the porosity of the relative large pores. Similar to the wireline electrical image, the isolated or developed fractures and vugs can be identified from LWD resistivity images (Figure 14).

In LWD, the GVR provides a conductivity map of the borehole wall, primarily from within the un-invaded zone. The classic Archie saturation equation is given as:

$$S_w^n = \frac{aR_w}{\Phi^m R_t} \quad (2)$$

By setting S_w = 1.0, a = 1.0 and m = n = 2.0, the Archie saturation equation can be written as:

$$\Phi = \frac{1}{S_w}\left(\frac{R_w}{R_t}\right)^{1/2} \quad (3)$$

This equation shows that once the porosity value of each depth is known, assuming the S_w and R_w are constant at each depth, any changes in formation resistivity (R_t) at a specific azimuth indicates the porosity (Φ) at that direction is varying.

For more accurate measurements, we concentrate on the focused azimuthal button resistivities. In each depth, the GVR provides 56 resistivity measurements around the borehole. Each resistivity measurement covers an azimuth of 6.4°; one vug may influence more than one azimuthal resistivity measurement, and at the same time one azimuthal resistivity may influence by multiple vugs (Figure 13). So the button resistivity measurement is not a simple average of azimuthal resistivity. One parameter is defined for this influence:

$$R_b = R_i \times V_m$$

Where R_b one button resistivity measurement, ohm.m
R_i one sector resistivity measurement, ohm.m
V_m Vug multiple effect factor, ohm.m

Replacing R_t with the button resistivity, the Archie Equation above can be transformed into:

$$\Phi = \frac{1}{S_w}\left(\frac{R_w}{R_i \times V_m}\right)^{1/2} \quad (4)$$

Applying the above equation, the GVR image can be transformed into a porosity map. Using the same methodology as used in PoroSpect (B.M Newberry, 1996), the secondary porosity can be analyzed.

From the result for A1H (Figure 17, 18), the secondary porosity developed zone can be analyzed. In low secondary porosity intervals, the external porosity and image-derived porosity is almost the same (Figure 17). The separation of these two porosities indicates the extent of secondary porosity development.

GEOMECHANIC ANALYSIS

In carbonate fractured reservoirs, hydrocarbon production is highly influenced by the fractures. Therefore, an understanding of fracture development is very important for carbonate reservoir evaluation. In general, fractures are associated with far field stress and local structural stress. Perhaps one group of fractures is controlled by far field stress, and another may be influenced by the local structure. Nevertheless, one set of fractures is generated by ancient stresses at a time. Moreover, the present far field stress may vary by different ancient stresses. Thus, finding fracture and stress relationships are the key element for fracture predication.

From the LWD resistivity image, there are two different types of fractures that can be identified; drilling-induced fractures and natural fractures. In most cases, the drilling-induced factures appear as a straight line with a corresponding line at 180° offset as shown in Figure19. The natural fractures generally show low apparent angles because of the high deviation of the horizontal wells as illustrated in Figure11. Normally, the strike of drilling-induced fractures reflects the maximum horizontal stress orientation. But considering the well trajectory with high deviation and NW-SE azimuth was similar to the present maximum horizontal stresses, the strike of the drilling-induced fractures is not the same as the present maximum horizontal stress.

According to the fracture statistics of these two wells, there are two sets of fractures identified in A2H, compared to one set found in A1H along the same strike (Figure 15); this NW-SE strike is same as the present maximum horizontal stress and is perhaps the reason for the fractures opening. The strike of another set of fractures is NEE-SWW and these closed fractures are found in the same direction as the major fault. The NEE-SWW strike fracture is not developed in A1H because of the larger displacement from a major fault.

Natural fractures exist in both wells, but in A2H the fractures are more developed in the tight zones compared to A1H. There are two sets of natural fractures; one is controlled by existing far field stresses, and the other is controlled by a major fault.

CONCLUSIONS

Quantitative analysis of fractures is possible by applying the dual laterolog resistivity methodology using GVR multiple depth button measurements. This method allows this novel means of fracture evaluation to be done using LWD measurements.

Secondary porosity is the key to understanding the heterogeneity of a carbonate reservoir. Although the GVR has a lower resolution compared to wireline resistivity images, the secondary porosity from the

GVR image can successfully be used to provide the means of understanding the complexity of a carbonate reservoir.

From GVR images, natural fractures, drilling induced fractures or borehole breakouts can be distinguished. By recognizing the different fracture types, the generation of natural fractures may be better understood and effectively used for natural fracture prediction.

With the combination of GVR resistivity images and ADN density and neutron data, a fully integrated formation evaluation can be carried out for lithological classification, geological applications and structural analysis. This provides the fundamentals for a thorough petrophysical and geomechanical analysis of the formation.

DISCUSSION

The fracture porosity from GVR multiple depth resistivities was not fully verified by core or production data. Nevertheless, the assumption made concerning resistivity separation is considered reasonable. For the moment, it only provides a qualitative analysis although with more data it should be possible to deliver a quantitative result.

The secondary porosity computation from GVR images can be used to evaluate the porosity texture, but this does not mean that the absolute value of the secondary porosity is the same as that obtained from core data. Furthermore, the selection of V_m is another variable that influences secondary porosity computation. We can only adjust V_m by checking the standard deviation of the input porosity and images obtained in shale or un-fractured tight zones, where the standard deviation should be as small as possible.

ACKNOWLEDGMENTS

We thank China National Offshore Oil Corporation for permission to present this material. We would also like to thank Tom Neville, Geoff Weller, Jeffrey Kok and Wu Bai Lin for their help and support during this work.

REFERENCES

Akinsanmi O.B., Aibangbe O and Kienitz C. "Application of Azimuthal Density While Drilling Images for Dips, Facies and Reservoir Characterization-Niger/Delta Expericence" SPE 65113 presented at SPE European petroleum Conference, Paris France, 24-25 October, 2000.

Evans M., et al., "Improved Formation Evaluation Using Azimuthal Porosity Data While Drilling" SPE 30546 presented at SPE annual technical conference & exhibition, Dallas, 22-25 October, 1995.

Ford G., et al., 1999, "Dip Interpretation from Resistivity at Bit Images (RAB) Provides a New and Efficient Method for Evaluating Sturcturally Complex Areas in the Cook Inlet, Alaska," SPE 54611, SPE Western Regional Meeting, Anchorage, Alaska, 26-28 May, 1999.

Greiss R-M, et al., 2003, "Real-time Density and Gamma Ray Images Acquired While Drilling Help to Position Horizontal Wells in a Structurally Complex North Sea Field," SPWLA 44th Annual Logging Symposium, June 22-25, 2003.

Newberry B.M., Grace L.M., and Stief D.D., "Analysis of Carbonate Dual Porosity Systems from Borehole Electrical Images" SPE 35158 presented at the Permian Basin Oil & gas recovery Conference, Midland Texas 27-29 March, 1996.

Pezard P.A., Anderson R.N., "In Situ Measurements of Electrical Resistivity, Formation Anisotropy, and Tectonic Context pyilippe", presented at SPWLA thirty-first Annual Logging Symposium, June 24-27, 1990.

Rosthal R.A., et al., "Formation Evaluation and Geological Interpretation from the Resistivity-at-the - Bit Tool," SPE 30550, SPE Annual Technical Conference & Exhibition, Dallas, USA, 22-25 October, 1995.

Sibbit A.M. & Faivare O., "The dual laterolog response in fractured rocks" presented at SPWLA twenty-sixth annual logging symposium, 17-20 June, 1985.

ABOUT THE AUTHORS

Lei Xiao is a senior reservoir engineer and Beibu Gulf exploration and development project manger of CCLZ.

Cai Jun is a Senior Petrophysicist and Petrophysics supervisor of CCLZ exploration and development department, take responsibility of new wireline and LWD technology applications.

Yang Shi Duo is a Senior Geologist and Geologist Domain Champion with Schlumberger for China, Korea & Japan. He graduated with B.A in Geology and B.A in Computer science from Petroleum University of China in 1995.

Shim Yen Han is a Senior LWD Petrophysicist and LWD Domain Champion with Schlumberger for China, Korea & Japan. She holds a Petroleum Engineering degree from University Technology of Malaysia.

Wu Hong Xia is a Geologist in Data Consulting Service segment Schlumberger, Beijing.

Wang Yu Xi is a Senior Petrophysicist in Data Consulting Service segment Schlumberger, Beijing.

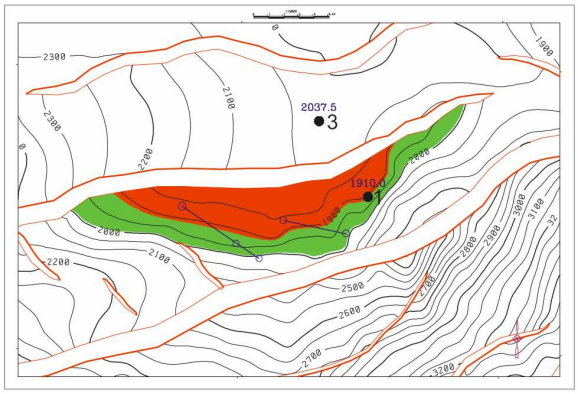

Figure 1: *Top Carboniferous structure map.*

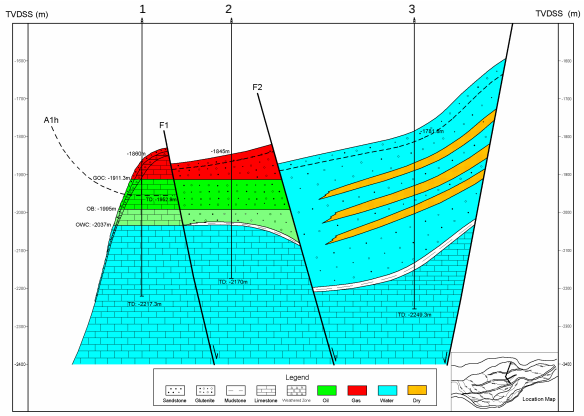

Figure 2: *Reservoir cross section map showing position of the three exploration wells.*

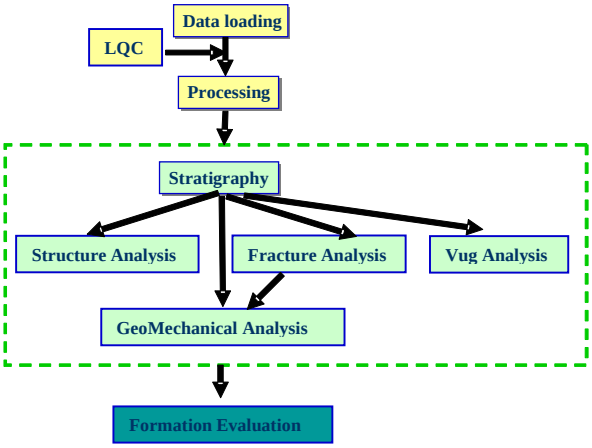

Figure 3: *LWD resistivity image processing and interpretation workflow.*

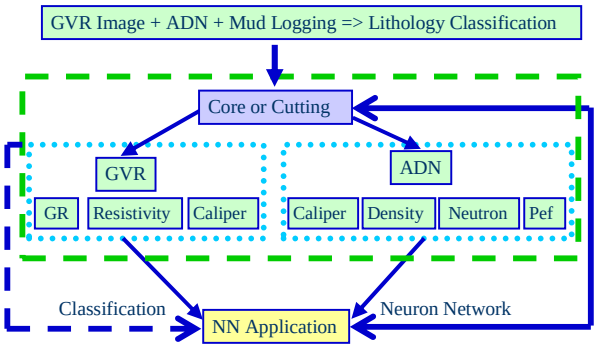

Figure 4: *Lithology classification methodology.*

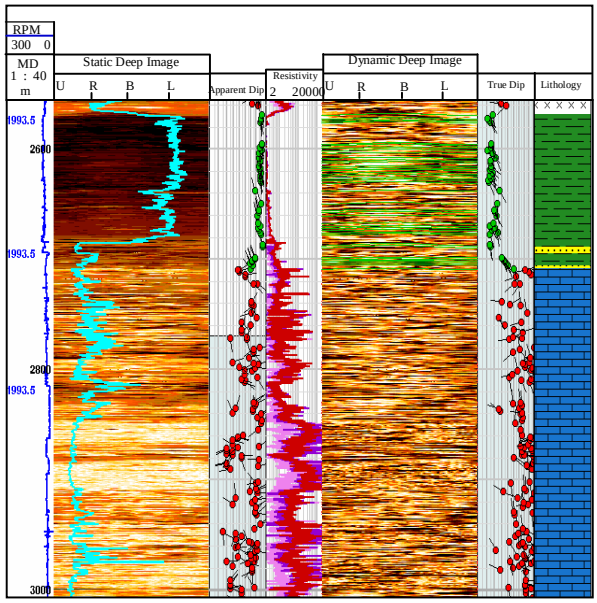

Figure 5: *A2h well lithology classification using LWD resistivity image.*

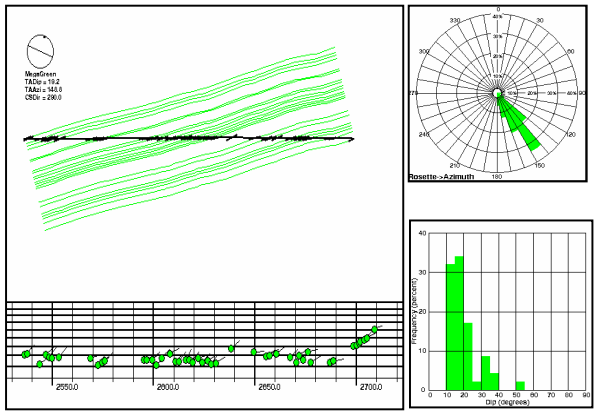

Figure 6: *A2H structure cross section, azimuth and dips.*

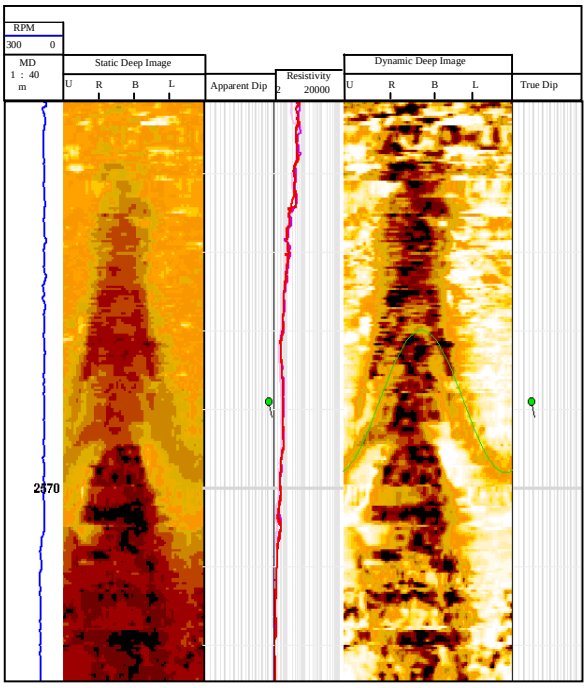

Figure 7: *Bed boundary in GVR image. The green tadpole corresponds to formation bed boundaries.*

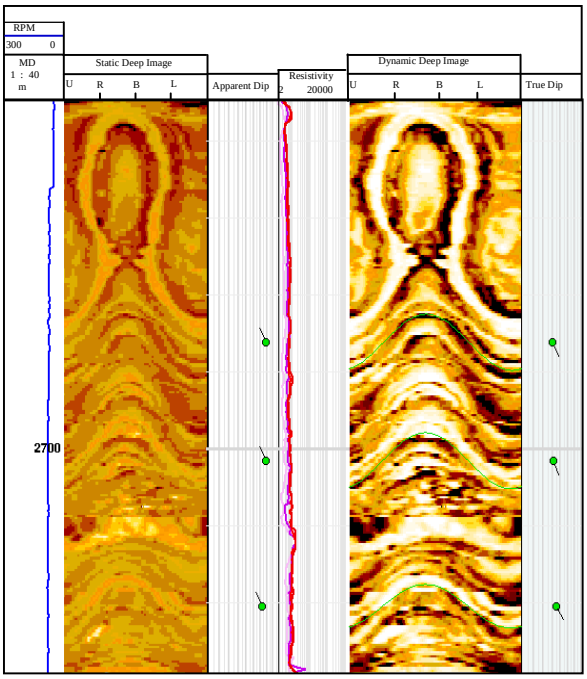

Figure 9: *Deformation features in LWD resistivity image.*

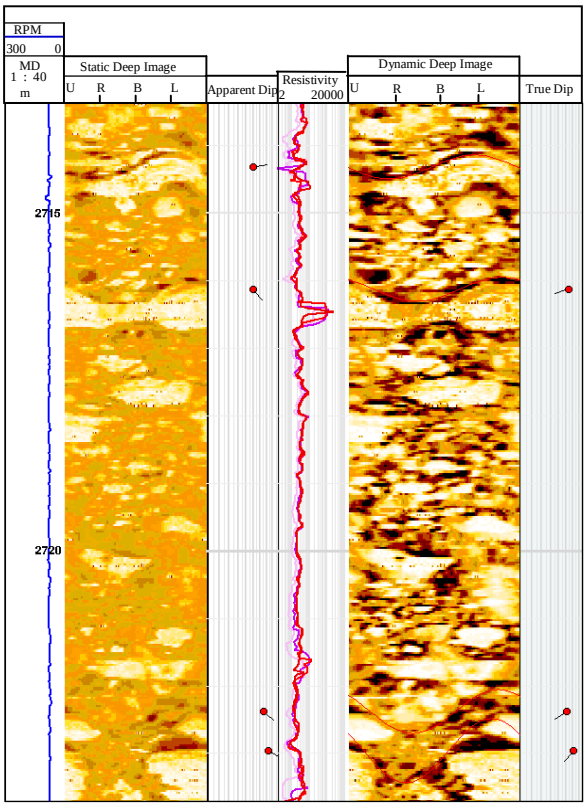

Figure 8: *Breccia zone features in GVR image. The red tadpoles correspond to fractures.*

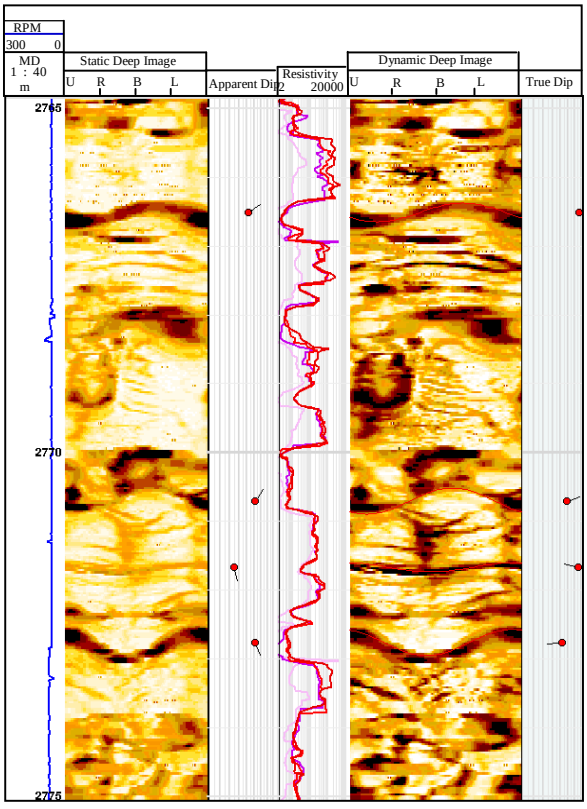

Figure 10: *Fractured carbonate zone with interbedded tight features.*

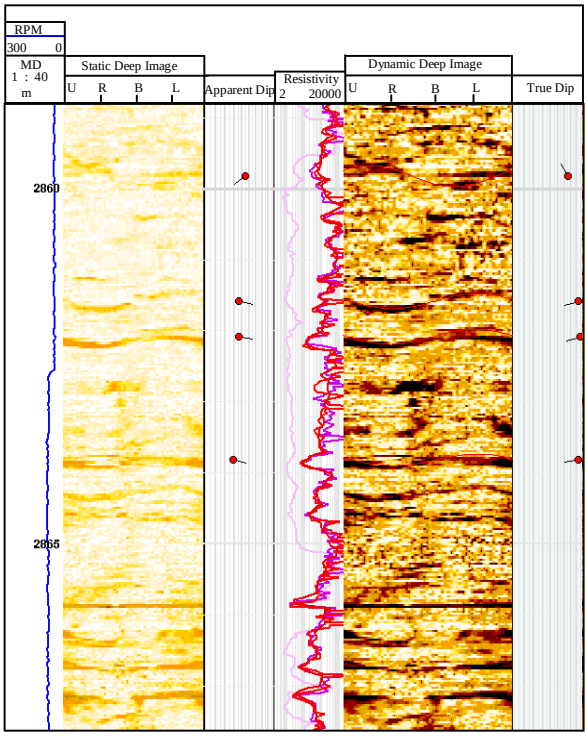

Figure 11: *Fractured carbonate features in LWD resistivity image.*

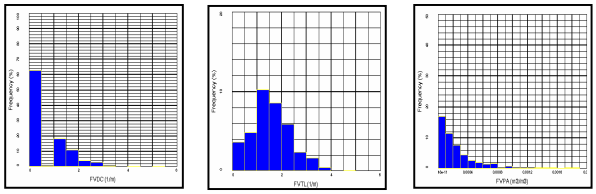

FVDC <5.202#/m (0.606) | FVTL <4.633/m (1.578) | FVPA <0.19 %(0.03)

Figure 12: *Fracture parameters statistics.*

Figure 13: *Vug multiple effect factor.*

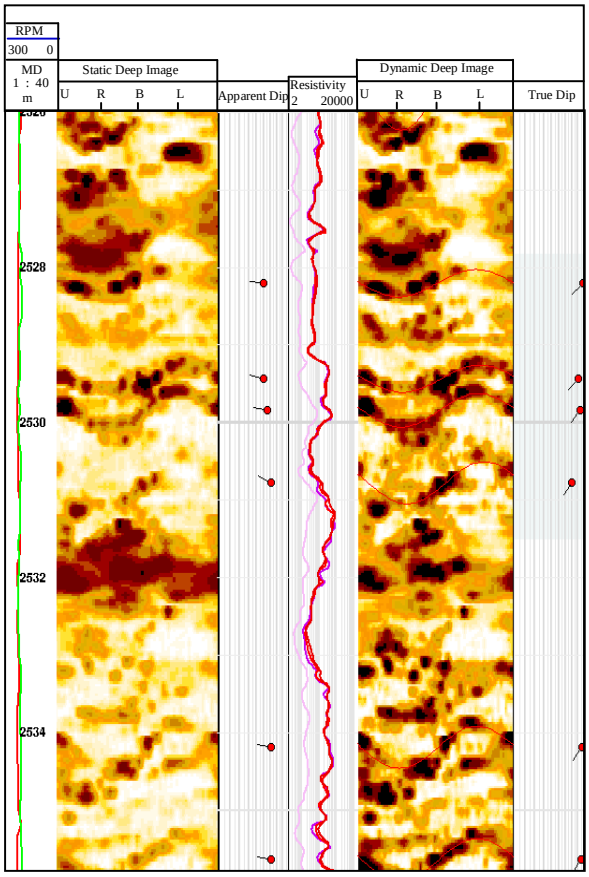

Figure 14: *Vugs appear as darker features in LWD resistivity image features.*

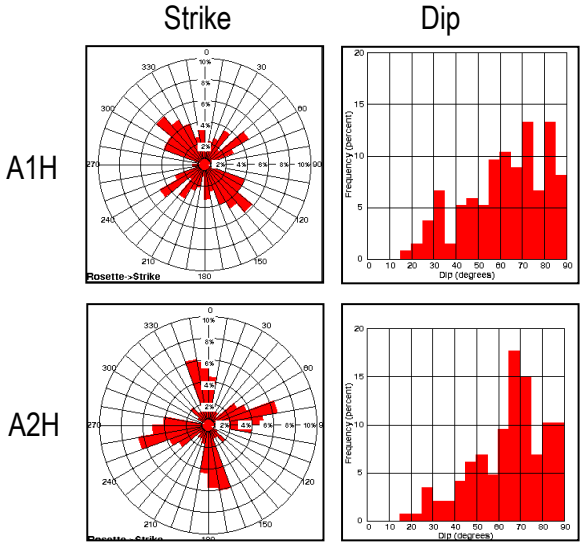

Figure 15: *Fracture strike and dip statistics.*

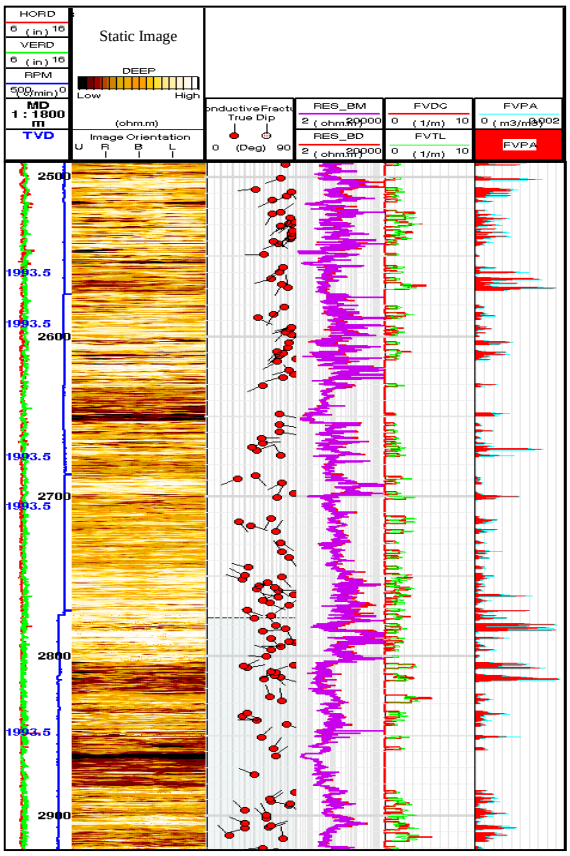

Figure 16: *Fracture quantitative calculation result.*

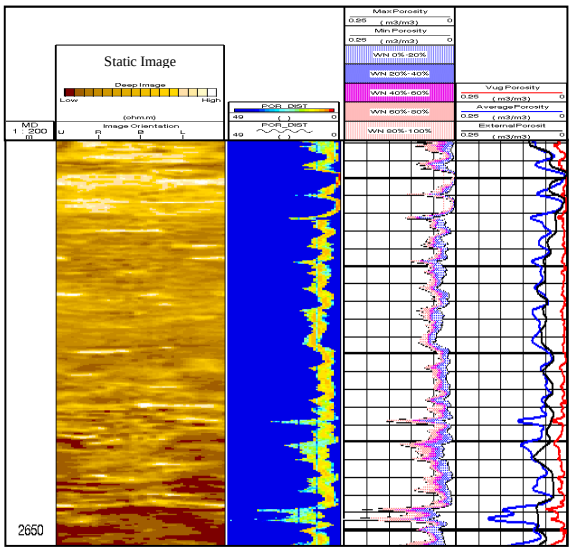

Figure 17: *A1H low secondary porosity interval. Track 2 displays GVR static deep button resistivity image, Track 3 & 4 shows porosity distribution spectrum, while track 5 shows the external porosity(black), image-derived porosity (blue) and secondary porosity (red).*

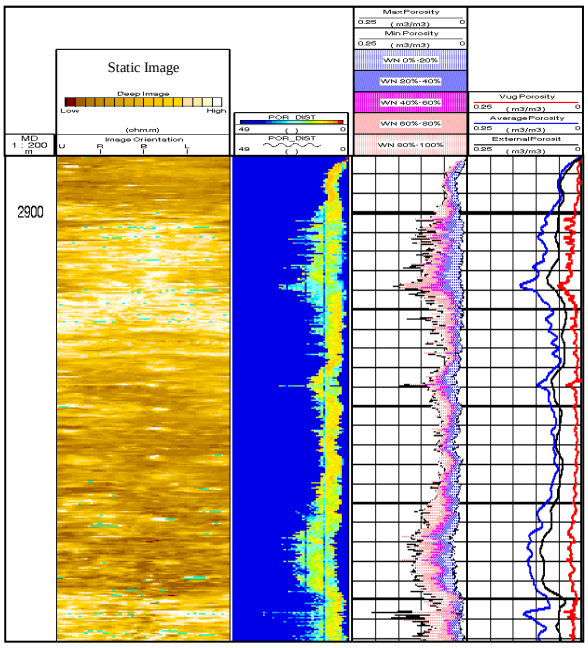

Figure 18: *A1H high secondary porosity interval.*

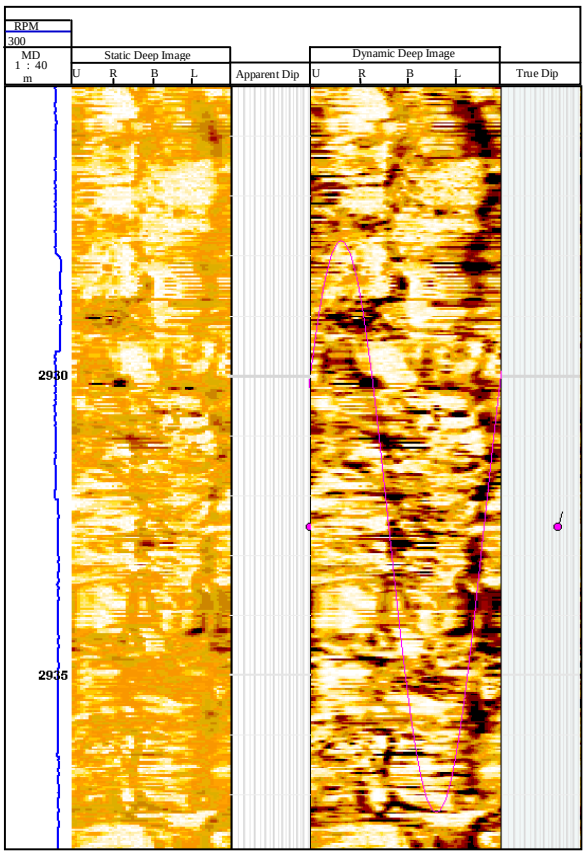

Figure 19: *Drilling-induced fracture in LWD image. The pink tadpole corresponds to drilling- induced fractures.*